Dystroglycan is selectively cleaved at the parenchymal basement membrane at sites of leukocyte extravasation in experimental autoimmune encephalomyelitis

Smriti Agrawal,[1] Per Anderson,[2] Madeleine Durbeej,[3] Nico van Rooijen,[4] Fredrik Ivars,[2] Ghislain Opdenakker,[5] and Lydia M. Sorokin[1,6]

[1]Experimental Pathology, [2]Immunology, and [3]Experimental Medical Science, Lund University, Lund 22185, Sweden
[4]Vrije Universiteit, Molecular Cell Biology, 1081 BT Amsterdam, Netherlands
[5]Immunobiology, Rega Institute for Medical Research, University of Leuven, B-3000 Leuven, Belgium
[6]Institute for Physiological Chemistry and Pathobiochemistry, Münster University, 48149 Münster, Germany

The endothelial cell monolayer of cerebral vessels and its basement membrane (BM) are ensheathed by the astrocyte endfeet, the leptomeningeal cells, and their associated parenchymal BM, all of which contribute to establishment of the blood–brain barrier (BBB). As a consequence of this unique structure, leukocyte penetration of cerebral vessels is a multistep event. In mouse experimental autoimmune encephalomyelitis (EAE), a widely used central nervous system inflammatory model, leukocytes first penetrate the endothelial cell monolayer and underlying BM using integrin β1–mediated processes, but mechanisms used to penetrate the second barrier defined by the parenchymal BM and glia limitans remain uninvestigated. We show here that macrophage-derived gelatinase (matrix metalloproteinase [MMP]-2 and MMP-9) activity is crucial for leukocyte penetration of the parenchymal BM. Dystroglycan, a transmembrane receptor that anchors astrocyte endfeet to the parenchymal BM via high affinity interactions with laminins 1 and 2, perlecan and agrin, is identified as a specific substrate of MMP-2 and MMP-9. Ablation of both MMP-2 and MMP-9 in double knockout mice confers resistance to EAE by inhibiting dystroglycan cleavage and preventing leukocyte infiltration. This is the first description of selective in situ proteolytic damage of a BBB-specific molecule at sites of leukocyte infiltration.

CORRESPONDENCE
Lydia M. Sorokin:
sorokin@uni-muenster.de

Abbreviations used: BBB, blood–brain barrier; BM, basement membrane; CNS, central nervous system; DKO, double KO; EAE, experimental autoimmune encephalomyelitis; GFAP, glial fibrillary acidic protein; MMP, matrix metalloproteinase; MOG, myelin/oligodendrocyte glycoprotein; WGA, wheat germ agglutinin.

The migration of leukocytes through interstitial extracellular matrices has recently received considerable attention. Sophisticated in vitro assays using fibrous collagen matrices and three-dimensional investigation of leukocyte migration suggest a β1-integrin– and protease-independent mode of leukocyte movement within interstitial matrices (1). Although these studies are physiologically more relevant than studies of random migration on or through immobilized substrates, they do not reflect the complexity of the in vivo situation nor are they relevant to the specialized migration processes required to cross basement membranes (BMs). The BM is the first barrier encountered by emigrating leukocytes subsequent to penetration of the vascular endothelial monolayer. Transmigration of this barrier remains difficult to investigate in vitro and the most physiological studies use in vivo inflammatory models (2, 3) or intravital approaches (4).

BMs are tight assemblies of specialized extracellular matrix molecules. Together with the endothelial cell monolayer, the BM presents a barrier to the movement of proteins and cells across the blood vessel wall. Our work has shown that blood vessel endothelium has a specialized BM characterized by the presence of two laminin isoforms, laminins 8 and 10 (5). Studies by Karnovsky et al. were the first to demonstrate that central nervous system (CNS) vessels are particularly impermeable to the movement of small molecules and elucidated the ultrastructural basis of this blood–brain barrier (BBB) (6). Post-capillary venules in the CNS are ensheathed by a second BM known as the parenchymal BM, produced by the astrocytes and associated leptomeningeal cells (6), which is characterized by presence of laminins 1 and 2 (5). A similar differential expression of cellular receptors for extracellular matrix

molecules at the endothelial and parenchymal borders also exists. In particular, dystroglycan is exclusively expressed on the astrocyte endfeet (5, 7, 8). Dystroglycan exists as an extracellular α-subunit and a transmembrane β-subunit, which are products of the same gene and result from posttranslation processing of the molecule (9). The α-dystroglycan subunit is a receptor for several BM components of the parenchymal BM, including laminins 1 and 2, perlecan and agrin (10), as well as the extracellular neuronal component, neurexin (11), and is considered to anchor the astrocyte endfeet to the parenchymal BM. Collectively, the endothelial cell layer, astrocyte endfeet, and their associated BMs constitute the cellular BBB and defects in any one of these components compromises the barrier function of CNS vessels (11, 12).

Using a mouse model of experimental autoimmune encephalomyelitis (EAE), we have shown that encephalitogenic T cells interact with the endothelial BM laminins, but not with the parenchymal BM laminins, despite having the cellular receptors capable of mediating such interactions (5). In the course of EAE, leukocytes accumulate in the perivascular space defined by the inner endothelial BM and the outer parenchymal BM, leading to focal leukocyte accumulation known as perivascular cuffs. Clinical symptoms, however, only become apparent after leukocyte penetration of the parenchymal BM. These results indicate that the mechanism of leukocyte transmigration of the inner endothelial cell BM differs from that used to penetrate the parenchymal BM and that the latter is a disease-relevant step. A delay in the onset of EAE symptoms has been observed in several mouse strains, some of which suggest a delay in the penetration of the outer parenchymal border. These include macrophage-depleted mice (13), TNF-α KO mice (14), and L-selectin KO mice (15). In the macrophage-depleted mice, leukocyte transendothelial cell migration is not impeded, but rather deficiencies occur at the level of transmigration of the parenchymal BM and the glia limitans, supporting the concept of a double barrier migration process (13). Passive transfer of encephalitogenic T cells in macrophage-depleted mice results in T cell accumulation in the perivascular cuff, suggesting that macrophages have a primary role associated with penetration of the parenchymal BM and infiltration of the CNS parenchyma (13).

The initial transmigration of the endothelial monolayer requires expression of the adhesion molecule α4 integrin by leukocytes (3). Integrin α4β1 binds to vascular cell adhesion molecule-1 on the endothelial surface in inflamed vessels and induces matrix metalloproteinase-2 (MMP-2) expression in encephalitogenic T cells, which has been proposed to facilitate transmigration of the subendothelial matrix (16). MMPs are a family of Zn^{2+}-dependent endopeptidases that degrade extracellular matrix proteins, but also CNS proteins such as myelin basic protein (17), NG2 proteoglycan (18), and cytokines and chemokines (19–21). MMPs are expressed during embryonic development and in pathological situations where tissue remodeling occurs. They are synthesized in an inactive proform that is activated extracellularly by proteolytic cleavage under the regulation of several inflammatory mediators, including cytokines and chemokines. MMPs have been extensively studied in multiple sclerosis and EAE, demonstrating activity of MMP-14/MMP-2 (16) and MMP-9 (22), and possibly also of MMP-7 (23) and MMP-8 (24). However, whether and which MMPs affect inflammatory cell entry into the parenchyma of the CNS or demyelination remains unclear. Although protease inhibitors reduce the severity or delay the onset of EAE, to date no protease inhibitor has been shown to completely ablate leukocyte migration into the perivascular space or into the brain parenchyma (25, 26). As a result of the hitherto lack of consideration of the cellular and BM barriers encountered by emigrating leukocytes, it is also unclear whether the main targets of MMP activity are components of the endothelial cell layer or the parenchymal border.

The aim of this study is to define sites of protease activity in the course of leukocyte infiltration into the CNS in a mouse EAE model and to identify potential targets of enzyme activity. The study uses a combination of in situ zymography and immunofluorescence, permitting simultaneous identification of sites of protease activity and endothelial and parenchymal BMs, as well as infiltrating leukocytes. The gelatinases MMP-2 and MMP-9 were identified as the major proteases active at sites of leukocyte infiltration into the brain parenchyma, subjacent to the parenchymal BM. Macrophages were shown to be major sources of MMP-2 and MMP-9, and dystroglycan, which acts to anchor astrocyte endfeet to the parenchymal BM, was identified as a novel target of this gelatinase activity. Genetic elimination of both MMP-2 and MMP-9 resulted in resistance to EAE and absence of both dystroglycan cleavage and leukocyte infiltration into the CNS. The data reinforce the concept that leukocyte transmigration of the inner endothelial and outer parenchymal BMs are separate events involving distinct molecular mechanisms, and demonstrate that selective gelatinase activity is essential for leukocyte penetration of the outer parenchymal barrier. This is the first report of selective alteration of a molecule expressed at the BBB at sites of leukocyte penetration and it introduces the possibility that control of gelatinase activity may restrict leukocyte infiltration and thereby block onset of EAE symptoms.

RESULTS

In situ and gel zymography

To define sites of protease activity, in situ zymography was performed on stage 2 and 4 EAE brain sections using either fluorescein-conjugated gelatin or collagen type IV as substrates. This was combined with immunofluorescent staining with a pan-laminin antibody to identify the endothelial and parenchymal BMs, or with CD45 to localize sites of leukocyte infiltration (Fig. 1, A and B). Activity was detected when gelatin (Fig. 1, C–F) and not collagen type IV (Fig. 1 G) was used as substrate, indicating gelatinase and not collagenase activity. Gelatinase activity was focused at sites of leukocyte infiltration into the brain parenchyma, subjacent to the

parenchymal BM (Fig. 1, C–F), and was abolished by the general MMP inhibitor, 1,10-phenanthroline (Fig. 1 H).

As no antibodies exist that recognize active gelatinases (MMP-2 and MMP-9) in inflamed mouse tissues, gel zymography was used to identify gelatinases present in EAE brains. Results revealed prominent bands at ~70 and 100 kD in EAE but not noninflamed brain extracts (Fig. 1 I). Comparisons with rMMP standards indicated that these bands represent the pro- and active forms of MMP-9 and MMP-2, respectively; suggesting that the gelatinase activity observed in in situ zymographies was MMP-2 and MMP-9. Weaker zymolytic bands of higher mol wt were apparent in EAE brain extracts (Fig. 1 I), indicating the presence of small amounts of neutrophil gelatinase B–associated lipocalin complexes (27).

Gelatinase substrates

As in situ zymography identified the parenchymal BM–astrocyte endfeet interface as the major site of MMP activity, investigation for MMP substrates was focused on this site. Immunofluorescence staining patterns and/or Western blots of extracellular matrix molecules and their cellular receptors (Table I) were investigated in EAE brains (stages 2 and 4). No change in the distribution or Western blot patterns was noted for most of the molecules investigated with the exception of dystroglycan.

Immunofluorescence staining of noninflamed vessels for β-dystroglycan and pan-laminin showed the occurrence of β-dystroglycan on astrocyte endfeet adjacent to the parenchymal BM, but not on vascular endothelium (Fig. 2, A–C). This pattern is clearer in inflamed vessels where endothelial and parenchymal BM are separated by the perivascular cuff (Fig. 2, D and E). At sites of leukocyte infiltration, β-dystroglycan staining was markedly reduced or absent (Fig. 2, E and G). We have previously shown the absence of discontinuities in the immunofluorescent staining pattern for integrin β1 on the astrocyte endfeet in EAE (5), suggesting that astrocyte endfeet are present at sites of leukocyte infiltration. This was confirmed by double staining for β-dystroglycan and glial fibrillary acidic protein (GFAP), as an astrocyte marker, which revealed no difference between GFAP staining of inflamed vessels that lacked β-dystroglycan staining and those that retained β-dystroglycan staining and had no sign of leukocyte infiltration (Fig. 2 F).

Dystroglycan binds to several parenchymal BM components, including laminins 1 and 2, agrin and perlecan. Loss of laminin 2 (28) or perlecan (29) from BMs have been reported to lead to instability of the dystroglycan receptor complex and its loss from the cell membrane. Examination of different stage EAE brains, triple or double immunofluorescently stained for dystroglycan, CD45 and laminin 1 (Fig. 2, G–I), laminin 2 (not depicted), agrin (Fig. 2, J and K), or perlecan (Fig. 2 L) revealed no discontinuity in these parenchymal BM components. As the result of lack of a suitable antibody, neurexin (another major dystroglycan ligand) was investigated only by Western blot analysis (see next paragraph).

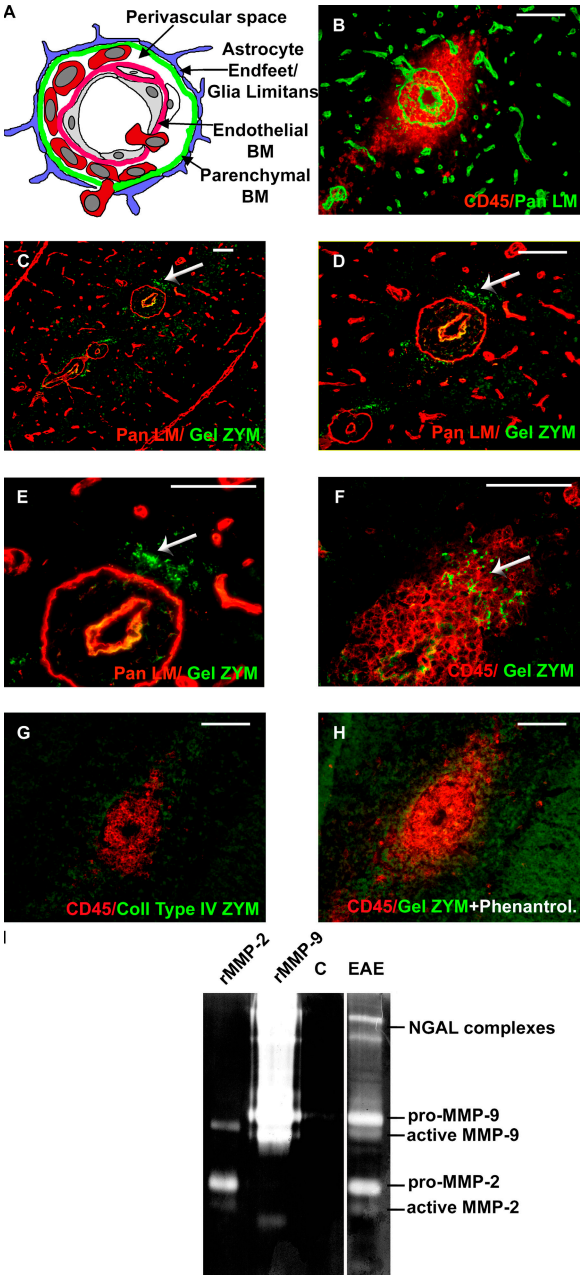

Figure 1. Gelatinase activity in EAE brains. Scheme of a post-capillary venule, showing cell layers and endothelial and parenchymal BMs separated by the perivascular space (A). EAE brain sections stained for pan-laminin and CD45 show leukocyte accumulation in the perivascular space and infiltration into the brain parenchyma (B). In situ zymography coupled with pan-laminin (C–E) or CD45 (F) immunofluorescence reveals protease activity in the CNS parenchyma subjacent to the parenchymal BM (arrows) at sites of leukocyte infiltration, only when gelatin (C–F) and not collagen type IV (G) is used as substrate. 1,10-phenanthroline abolishes gelatinase activity (H). (I) Gelatin gel zymography of healthy (C) and EAE brains shows proforms of MMP-9 and MMP-2 and the smaller active forms in EAE samples only. Higher mol wt bands are neutrophil gelatinase B–associated lipocalin (NGAL)–associated lipocalin complexes. rMMP-2 and rMMP-9 are standards. C–E are the same specimen at different magnifications; B, C–E, and F–H are serial sections. Data represent results from 10 mice. Bars, 40 μm.

Table I. Primary antibodies to extracellular matrix molecules, their receptors, and cellular markers

Molecule	Antibody name/clone	Used in immunofluorescence (IF), Western blot (WB), or FACS	Reference/source
Laminin α1	317	IF, WB	(5)
Laminin α2	401	IF, WB	(5)
Laminin α4	377	IF, WB	(5)
Laminin α5	405	IF, WB	(5)
Laminin γ1	3E10	IF	(5)
Laminin β1	3A4	IF	(5)
Pan-laminin	455	IF, WB	(5)
Perlecan core	C11L1, A7L6	IF, WB	BD Biosciences
Brain-specific neurexin	Clone 17	WB	BD Biosciences
Collagen IV	R94.4	IF	(5)
Agrin	204	IF, WB	(48)
β-dystroglycan	VIMSA	IF, WB	(49)
β-dystroglycan	NCL-43DAG	WB	Novo Castra
α-dystroglycan	IIH6	WB	Upstate
β1 integrin	Ha2/5	IF	BD Biosciences
α6 integrin	GoH3	IF	BD Biosciences
GFAP	G-A-5	IF	Sigma-Aldrich
CD45.2	30F11	IF, FACS	BD Biosciences
CD11c	N418	FACS	BD Biosciences
DEC-205	NLDC-145	IF	Serotec
TCRβ	H57-587	IF, FACS	BD Biosciences
CD11b, CD107b	MAC1 (M1/70), MAC3 (M3/84)	IF, FACS, FACS	BD Biosciences, Serotec
GR-1	5C6	IF	Serotec

Interestingly, double staining for perlecan core protein and pan-laminin revealed a consistently stronger staining for perlecan in endothelial BMs than in parenchymal BMs (Fig. 2 L). The absence of β-dystroglycan staining and the differential perlecan staining in endothelial versus parenchymal BMs was not the result of epitope masking, as both general unmasking techniques and treatment with heparatinase or hyaluronidase did not alter this pattern.

To investigate possible proteolytic cleavage not detectable by immunofluorescence, Western blots were performed for agrin, laminins 1 and 2, and neurexin. Crude stage 4 EAE brain extracts revealed no indication of proteolytic cleavage of agrin, laminin 1, and neurexin (agrin shown in Fig. 2 M).

Western blot analysis of glycoprotein-enriched extracts from EAE and non-EAE brains revealed the intact β-dystroglycan molecule at 43 kD in all samples, and an additional 30-kD cleavage fragment in EAE samples only (Fig. 3 A). β-dystroglycan is a transmembrane molecule that is covalently bound to an extracellular α-dystroglycan subunit. Western blot analysis of plasma membrane preparations from EAE brains demonstrated that the 30-kD β-dystroglycan fragment is retained in the cell membrane of the astrocyte endfeet (Fig. 3 B). No evidence of proteolytic cleavage of α-dystroglycan was apparent and only the intact molecule of 120 kD was detected in EAE brains (Fig. 3 C); lower bands in Fig. 3 C are nonspecific cross-reactivity of the secondary antibody with μ chains of endogenous IgM (abundant in inflamed brains) as shown in the negative control (Fig. 3 D).

To test whether MMP-2 and/or MMP-9 were responsible for cleavage of β-dystroglycan in the EAE brains, normal brain extracts were treated with activated rMMP-2 or rMMP-9. Fig. 4 A shows the presence of intact 43-kD β-dystroglycan and the 30-kD cleavage product in both MMP-2– and MMP-9–treated samples, identical to those observed in EAE brains. As other MMPs have been implicated in EAE, the ability of activated rMMP-1, rMMP-7, rMMP-8, and rMMP-3 to cleave dystroglycan from non-EAE brains was tested. Fig. 4 B shows that none of these MMPs cleave dystroglycan to the 30-kD fragment characteristic of EAE brain extracts.

Macrophages are major sources of gelatinases

Macrophages have been suggested as critical cell types in autoimmunity. Apart from their potential role as APC in EAE, macrophages have been suggested to have an additional role in the movement of T cells from the perivascular space into the brain parenchyma (13). When encephalitogenic T cells are adoptively transferred into macrophage-depleted mice, T cells accumulate in the perivascular space, but disease is not induced. As macrophages are also major producers of several MMPs (30), we investigated whether macrophages can produce MMP-2 and MMP-9 and whether they contribute to the selective cleavage of dystroglycan at the parenchymal

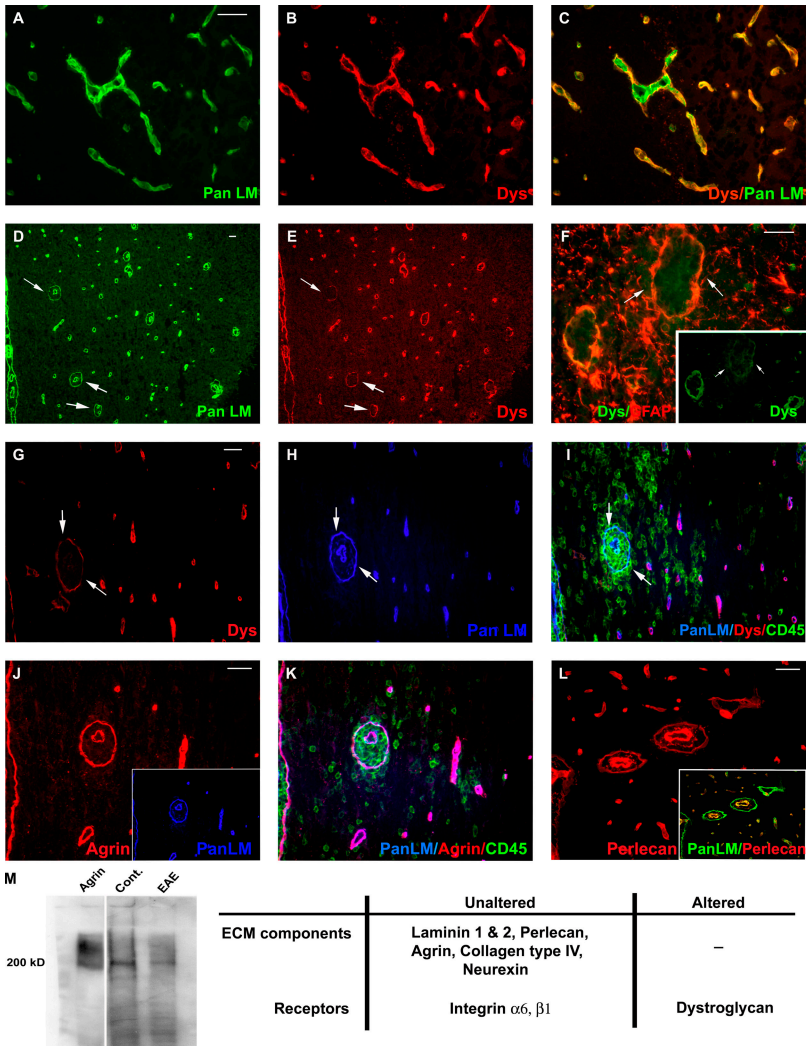

Figure 2. β-dystroglycan loss in inflamed vessels. Immunofluorescence for β-dystroglycan and pan-laminin reveals continuous β-dystroglycan staining bordering the parenchymal BM in noninflamed vessels (A–C) and loss of β-dystroglycan in inflamed vessels only (arrows in D and E). Triple staining for pan-laminin with β-dystroglycan and CD45 (G–I), or agrin and CD45 (J and K) reveals loss of β-dystroglycan at sites of leukocyte infiltration (G and I), despite continuous pan-laminin (H) and agrin (J and K) staining. Double β-dystroglycan and GFAP staining indicates presence of astrocyte endfeet surrounding inflamed vessels (arrows in F). Perlecan staining of the parenchymal BM is continuous around perivascular cuffs, with higher intensity staining in endothelial BMs (L). Western blot reveals ∼200 kD agrin core protein and the characteristic broad mol wt smear in stage 4 EAE and noninflamed brains (Cont.) and purified agrin (M). The table summarizes immunofluorescence and Western blot data. Images are from different specimens and represent results from 10 mice. Bars, 40 μm.

border. This involved EAE induction by myelin/oligodendrocyte glycoprotein (MOG) immunization in mice depleted of macrophages by treatment with clodronate-liposomes (13). Control mice were treated with PBS-liposomes or no liposomes.

EAE symptoms were apparent in mice treated with PBS-containing liposomes or no liposomes by day 10 after immunization, whereas clodronate-liposome–treated mice remained resistant to EAE up to day 20 after MOG immunization (Fig. 5 A). In EAE, $CD45^+$ T cells and monocyte/macrophages infiltrate the CNS and are recovered from perfused CNS tissues by discontinuous density gradient centrifugation and quantified by FACS (31). This extravasated $CD45^+$ population was examined in PBS- and clodronate-liposome–treated mice for $MAC3^{high}/CD45^{high}$ macrophages (31), $MAC3^{high}/CD45^{low}$ activated microglia (31), and $TCR\beta^+$ T cells (Table I). The total number of $CD45^+$ cells recruited to the CNS in clodronate-treated mice at day 19 was 30% of that observed in PBS-treated mice at day 15 or in clodronate-treated mice at day 21 after MOG immunization. A significantly lower proportion of these $CD45^+$ cells represented macrophages in the CNS of clodronate-treated mice at day 19 (13% ± 0.34), as compared with clodronate-treated mice at day 21 (28% ± 2.1) or mice treated with PBS-liposomes (32% ± 6.4) (Fig. 5 B). Proportions of T cells recruited to the CNS and proportions of activated microglia in the CNS were, however,

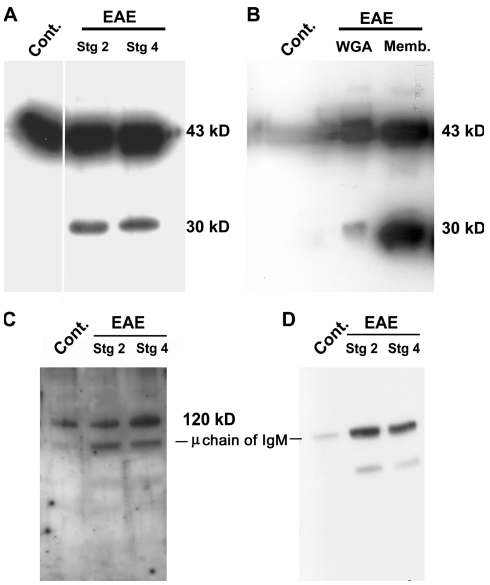

Figure 3. In vivo β-dystroglycan cleavage. Western blots for β- (A and B), α-dystroglycan (C), and secondary antibody control (D). A and C and WGA in B are glycoprotein-enriched CNS samples; Memb. is a CNS membrane fraction (B). All samples are run under reducing conditions. Intact β-dystroglycan at 43 kD is detected in stage 2 and 4 EAE and in noninflamed brains (Cont.) (A and B). An additional 30-kD β-dystroglycan fragment occurs only in EAE glycoprotein enriched and membrane fractions (A and B). Intact α-dystroglycan is observed at ~120 kD in all samples (C). Lower bands in C are nonspecific cross-reactivity of the secondary antibody (D). The ~80-kD band represents endogenous IgM μ chain, abundant in inflamed CNS, as shown in the negative control (D).

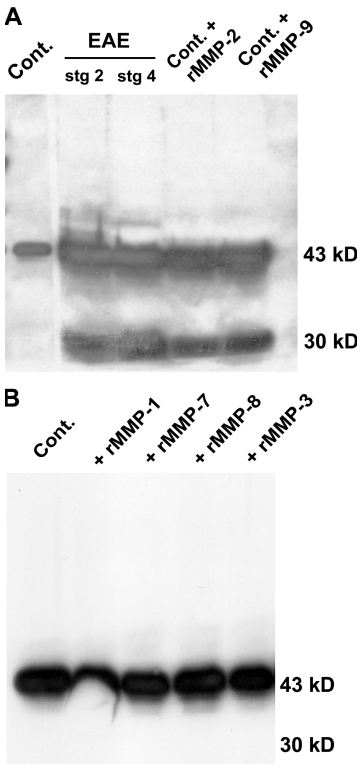

Figure 4. MMP-2 and MMP-9 cleave β-dystroglycan. Western blots for β-dystroglycan in glycoprotein-enriched samples from noninflamed brains (Cont.), stage 2 and 4 EAE brains, or Cont. samples treated with activated rMMP-2 or rMMP-9 result in the same 30-kD β-dystroglycan fragment as seen in EAE samples. Weak reaction of the secondary antibody with endogenous Ig as a result of serum influx into diseased brains is seen at ~50 kD (A). Treatment of the same noninflamed sample with activated rMMP-1, rMMP-7, rMMP-8, or MMP-3 does not cleave β-dystroglycan (B).

unaffected by clodronate treatment (Fig. 5 B). Previous studies have shown a specific reduction of the macrophage population in LN and spleens of clodronate-treated mice at day 2 after clodronate injection (32), which was confirmed here (unpublished data).

Immunofluorescence revealed that MAC3$^+$ macrophages were abundant in perivascular cuffs of PBS-liposome–treated mice, but were absent from clodronate-liposome–treated mice up to day 19 after MOG immunization (Fig. 5 B). Reappearance of macrophages in the CNS parenchyma of clodronate-liposome–treated mice at day 21 coincided with infiltration of CD45$^+$ leukocytes and appearance of clinical symptoms (Fig. 5 B). Infiltration of nonmacrophage, CD45$^+$ cells was still apparent surrounding vessels in areas outside of the brain parenchyma; e.g., within the choroid plexus and in the leptomeningeal space, in the clodronate-liposome–treated mice (unpublished data). Immunofluorescent staining identified these cells as T cells, DCs, and granulocytes, further confirming that development of the immune response was normal and that leukocyte recruitment to the CNS was not impaired, despite absence of infiltration into the CNS parenchyma. Absence of a general deficiency in T cell activation was also confirmed by in vitro T cell proliferation studies performed on clodronate- and PBS-liposome–treated mice at day 15 and, in the case of clodronate-liposome–treated mice, at days 19 and 21 after MOG immunization. Antigen-specific (MOG 35–55) (Fig. 6 A) and anti-CD3–induced (Fig. 6 B) T cell proliferation showed no significant difference between mice treated with clodronate- or PBS-liposomes. Hence, the data indicate that clodronate treatment specifically depletes macrophages and does not affect other leukocyte populations or microglia.

Gelatinase activity was not detectable in clodronate-liposome–treated mice up to day 19 after MOG immunization by in situ (Fig. 7 A) or gel zymography (Fig. 7 B). Corresponding immunofluorescence showed continuous β-dystroglycan staining surrounding post-capillary venules (Fig. 7 A) and Western blots revealed only intact 43-kD dystroglycan (Fig. 7 C). By day 21, gelatinase activity was detectable by in situ zymography (Fig. 7 A) and gel zymography revealed the presence of pro- and active MMP-2 and MMP-9 (Fig. 7 B). In situ zymography localized the gelatinase activity around post-capillary venules at sites of leukocyte penetration of the parenchymal border (Fig. 7 A), where β-dystroglycan staining was significantly reduced or absent (Fig. 7 A). Corresponding Western blots revealed the presence of the 30-kD

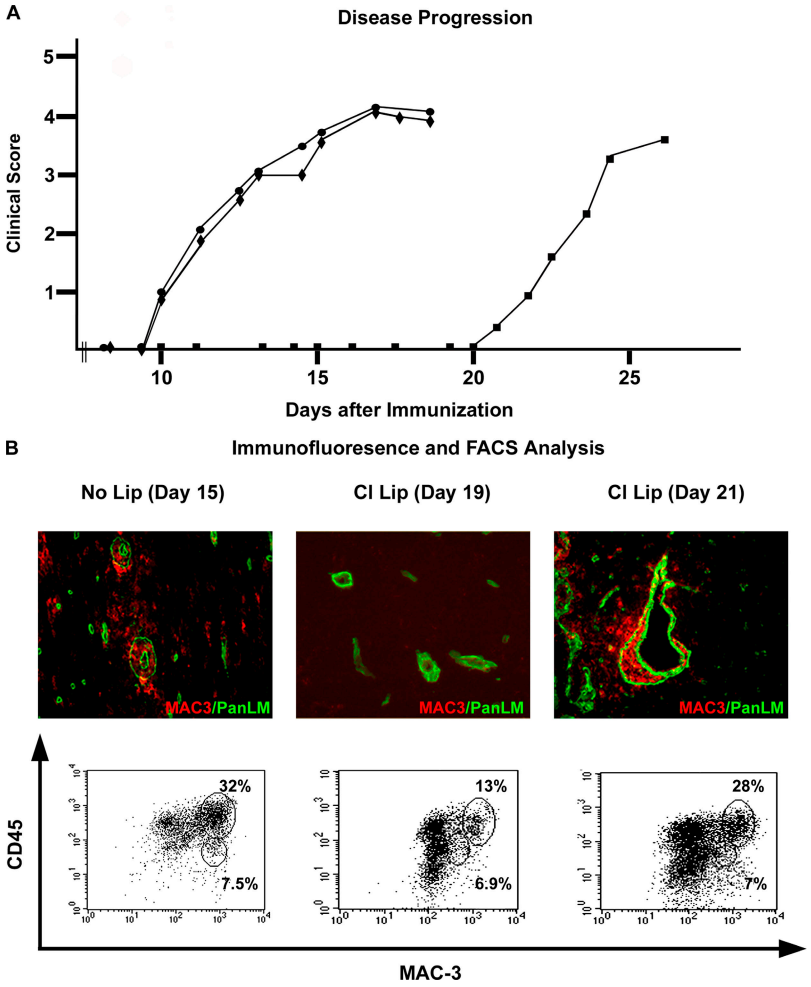

Figure 5. Macrophage depletion delays EAE onset. (A) Clodronate-liposome (Cl Lip) (■)–treated mice are resistant to EAE up to day 21 after MOG immunization, whereas clinical symptoms appear by day 10 in PBS-liposome (◆)–treated and untreated mice (●). (B) FACS of CNS infiltrates reveals that $CD45^{high}/MAC3^{high}$ macrophages represent 32% of the total $CD45^{+}$ population at day 15 after immunization and reduction of this population to 13% in Cl Lip–treated mice at day 19. By day 21, the proportion of $CD45^{high}/MAC3^{high}$ macrophages increases to 28% in Cl Lip–treated mice, coincident with EAE onset. Proportions of activated $CD45^{low}/MAC3^{high}$ microglia do not vary between groups (7.5, 6.9, 7%). Immunofluorescence reveals MAC3 positive macrophages in CNS parenchyma of PBS-liposome–treated mice at day 15 after immunization that are absent in Cl Lip–treated mice until day 19, reappearing at day 21. Images are from different mice and represent results from six mice in each group.

β-dystroglycan fragment only in brain extracts of clodronate treated mice at day 21 after MOG immunization and of the PBS-liposome–treated mice (Fig. 7 C).

Macrophage-derived gelatinases cleave astrocyte β-dystroglycan

The in vivo studies suggest that macrophages are the source of MMP-2 and MMP-9 in EAE brains, and that these gelatinases may be responsible for the cleavage of astrocyte-derived β-dystroglycan. To test this possibility directly, peritoneal macrophages and astrocytes were isolated and cultured in vitro. Conditioned medium from macrophage cultures were shown by gel zymography to contain pro- and active MMP-2 and MMP-9, whereas astrocyte cultures did not contain detectable gelatinase activity (Fig. 8 A). Western blots revealed the identical 43-kD β-dystroglycan molecule on cultured astrocytes (Fig. 8 B) as observed in noninflamed CNS extracts (Fig. 8 D), corresponding to the intact molecule. Coculture of macrophages and astrocytes or incubation of macrophage conditioned medium with astrocyte cultures resulted in the 30-kD β-dystroglycan fragment (Fig. 8 B). This cleavage was inhibited by MMP inhibitors (TIMP-1 and TIMP-4), but not by serine protease or cysteine protease inhibitors (AEBSF, E64, or Aprotinin) (Fig. 8 C). Addition of macrophage-conditioned medium to glycoprotein-enriched, noninflamed CNS extracts was also sufficient to result in the 30-kD β-dystroglycan fragment (Fig. 8 D).

MMP-2/MMP-9 double DK (DKO) mice are resistant to EAE

To investigate the correlation between MMP-2/MMP-9 activity, dystroglycan cleavage, and EAE induction, MMP-2 KO, MMP-9 KO, and MMP-2/MMP-9 DKO mice were

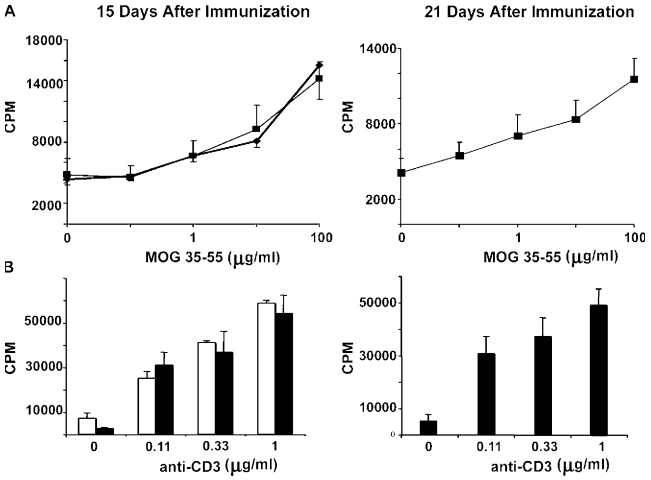

Figure 6. T cells proliferate normally in clodronate–liposome–treated mice. Antigen-specific (MOG 35–55) (A) and anti-CD3–induced T cell proliferation (B) show no significant difference between clodronate- (■ and black bars) or PBS-liposome (◆ and white bars)–treated mice at days 15 or 21 after MOG immunization. Data are means ± SEM from three experiments with $n = 3$.

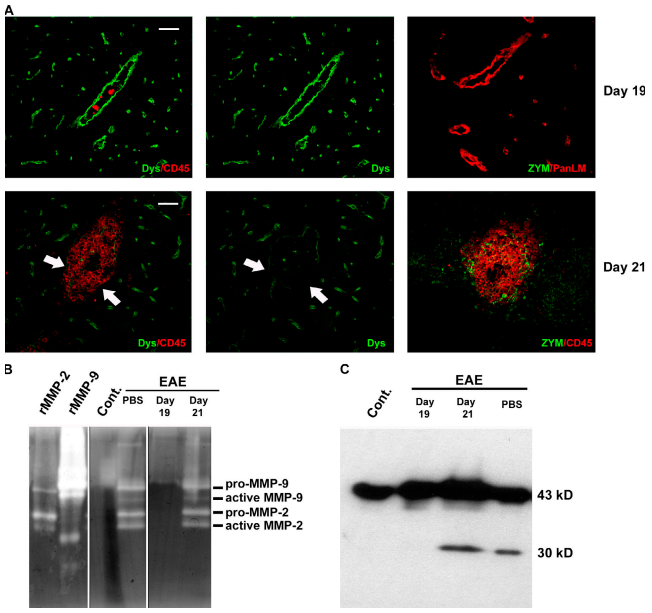

Figure 7. Macrophages are crucial for gelatinase activity and β-dystroglycan cleavage. (A) Immunofluorescence for CD45 and β-dystroglycan in CNS sections of clodronate-treated mice at days 19 and 21 after MOG immunization and corresponding gelatin in situ zymographies (ZYM) coupled with staining for CD45 or pan-laminin reveal loss of β-dystroglycan staining and gelatinase activity at the parenchymal border (arrows) only in brains of clodronate-liposome–treated mice at day 21. (B) Gelatin zymography reveals absence of MMP-2 and MMP-9 in CNS samples from noninflamed (Cont.) and clodronate-liposome–treated mice at day 19 after immunization, but not in PBS-liposome–treated mice or clodronate-treated mice at day 21. (C) Corresponding Western blots for β-dystroglycan reveal the 30-kD fragment in PBS-liposome–treated mice and clodronate-liposome–treated mice at day 21 after immunization, but not at day 19. Images in A are either the same section or serial sections and represent results from eight mice in each group. Bars, 40 μm.

used. Adult MMP-9-deficient mice have been previously shown to have no reduction in the onset or severity of EAE symptoms (22), which was confirmed here (Fig. 9 A). In MMP-2 KO mice used here, both onset of EAE symptoms and disease severity did not differ from +/− or WT littermates (Fig. 9 A and not depicted). In both MMP-2 KO and MMP-9 KO mice, immunofluorescence revealed the occurrence of perivascular cuffs and the loss of dystroglycan immunofluorescence at sites of leukocyte infiltration, whereas Western blots confirmed β-dystroglycan cleavage (Fig. 9, B and C). Cellular infiltrates were normal in both MMP-2 KO and MP-9 KO mice and consisted of macrophages, T cells, and DCs (Fig. 9 B). MMP-2/MMP-9 DKO mice showed no pro- or active forms of MMP-2 or MMP-9 in gel zymography (Fig. 9 A, inset). These DKO mice were resistant to EAE up to 40 d after MOG immunization; no $CD45^+$ T cell, macrophage, or DC infiltration was detected by immunofluorescence, whereas Western blots confirmed the absence of dystroglycan cleavage (Fig. 9, B and C). Single or double MMP-2 and MMP-9 +/− mice developed disease symptoms at ∼day 10 after immunization, similar to WT mice. Treatment of non-EAE brain tissue with macrophage-conditioned media resulted in cleavage of β-dystroglycan to the 30-kD product only when macrophages were derived from WT, MMP-2 KO, or MMP-9 KO mice, and not from MMP-2/MMP-9 DKO mice (Fig. 9 D).

DISCUSSION

Although MMPs have long been implicated in EAE (17), this is the first time that the combined inactivation of the gelatinases, MMP-2 and MMP-9, has been shown to be crucial for EAE resistance. Our data clearly show the presence of active gelatinases and not collagenases at sites of leukocyte infiltration, subjacent to the parenchymal BM, and associated focal loss of β-dystroglycan immunofluorescence. Western blot analysis revealed that the loss of β-dystroglycan staining was due to the result of its selective cleavage by both MMP-2 and MMP-9, resulting in a residual 30-kD transmembrane fragment and loss of the entire extracellular domain. This is the first identification of an in vivo MMP-2/MMP-9-specific substrate and the first description of selective in situ proteolytic damage of a BBB-specific molecule at sites of leukocyte infiltration.

Leukocyte infiltration into the CNS is a multistep process involving initial penetration of the endothelial monolayer and underlying BM, followed by temporary residency in the perivascular cuff bordered by the endothelial and parenchymal BMs, and finally migration across the parenchymal BM and glia limitans into the brain parenchyma. Our novel use of in situ zymography coupled with immunofluorescent staining for cellular and extracellular compartments of the inflamed vessels has allowed precise localization of protease activity in EAE. The data demonstrate that gelatinase activity

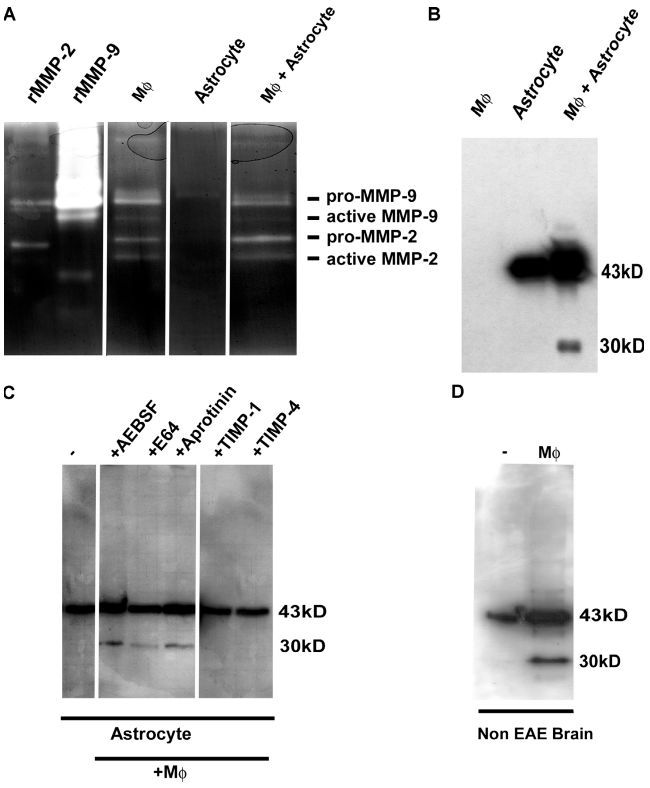

Figure 8. Macrophage-derived gelatinases cleave astrocyte and brain β-dystroglycan. (A) Gelatin zymography reveals pro- and active-MMP-2 and MMP-9 in macrophage-conditioned media (Mϕ), but not in astrocyte lysates. (B) Western blots reveal intact β-dystroglycan in astrocyte lysates, which is cleaved to the 30-kD fragment by addition of macrophage-conditioned media (Mϕ + astrocyte). (C) Cleavage of astrocyte-derived β-dystroglycan by macrophage-conditioned media is inhibited by MMP inhibitors (TIMP-1, TIMP-4), but not serine and cysteine protease inhibitors (AEBSF, E-64, Aprotinin). (D) Incubation of crude CNS extracts from healthy mice with macrophage-conditioned media is sufficient to cleave β-dystroglycan.

first becomes detectable in the perivascular space, which is the principal site of activity correlating with the sites of leukocyte migration across the parenchymal BM, and not with transmigration of the endothelial cell monolayer and its BM.

Gel zymography revealed that MMP-2 and MMP-9 are the major proteases active in the inflamed vessels, consistent with previous studies (16, 33), and that macrophages are a major source of these gelatinases. Macrophage depletion followed by active EAE induction revealed a tight correlation between the presence of macrophages and MMP-2 and MMP-9 activity and β-dystroglycan cleavage, whereas in vitro studies demonstrated that macrophage-derived MMP-2 and MMP-9 are sufficient for β-dystroglycan cleavage from the surface of astrocytes and are also capable of cleaving brain-derived β-dystroglycan. This strongly suggests that one role of macrophages in EAE is to provide active MMP-2 and MMP-9, which cleave β-dystroglycan at sites of leukocyte penetration of the parenchymal border. It is noteworthy that, contrary to our expectations, leukocytes did not accumulate in the perivascular cuff in macrophage-depleted mice, suggesting that macrophages have an additional role before their entry into the perivascular cuff that is independent of their proteolytic function. There is evidence that this additional role is likely to be antigen presentation (34). In the adoptive transfer model, a delay in T cell recruitment into the CNS occurs, which has been suggested to be the result of the time required for transferred T cells to be primed by recognition of CNS antigen in the periphery and then become competent to enter the brain parenchyma (35). Evidence exists for the involvement of both DCs and macrophages in this antigen presentation (34, 36). Our data show that macrophages are normally abundant in the leptomeningeal space and in perivascular cuffs in EAE and that clodronate-liposome treatment depletes these macrophage populations without affecting other antigen-presenting cells, such as DCs or activated microglia. Clodronate-liposome treatment also did not affect T cells or PMN, which were found to accumulate in the leptomeningeal space and in the choroid plexus, but did not infiltrate into the brain parenchyma, and T cell proliferation studies revealed that there was no major defect at the level of T cell activation. Our data, therefore, support an early role for macrophages in antigen presentation in EAE and suggest that this occurs before entry into the perivascular cuff, probably in the leptomeningeal space.

Despite strong gelatinase activity surrounding inflamed vessels, the observed selective cleavage of β-dystroglycan and the absence of significant proteolytic changes in the major endothelial or parenchymal BM components (such as laminins, collagen type IV, or agrin) argues against a general digestion of extracellular matrix barriers in EAE. Neurexin, a high affinity ligand for dystroglycan that occurs between neurons and not on the astrocyte endfeet (11), was also not affected, reflecting the spatial restriction of the gelatinase activity. Our data suggest that gelatinases are essential for selective cleavage events confined to the parenchymal BM–astrocyte endfeet border, which may lead to local permeability changes. This is substantiated by the fact that only localized extravasation of serum proteins occurs around inflammatory lesions and that this change in vessel permeability is a temporary event. β-dystroglycan is clearly one of the targets of this selective gelatinase activity. However, it cannot be ruled out that cleavage of BM components close to the amino- or carboxy-termini occurs, which may have profound impact on BM structure but are not detectable by the methods used here. The identification of such in vivo substrates for gelatinases remains difficult as a result of the temporally and spatially restricted action of gelatinases and low levels of cleaved fragments generated, but may become easier in the future with the development of novel mass spectrometry–based techniques (37).

The identification of β-dystroglycan as a novel in vivo substrate for MMP-2 and MMP-9 in EAE is the first report of a molecular alteration at the BBB associated with sites of leukocyte infiltration. The only other CNS protein that has

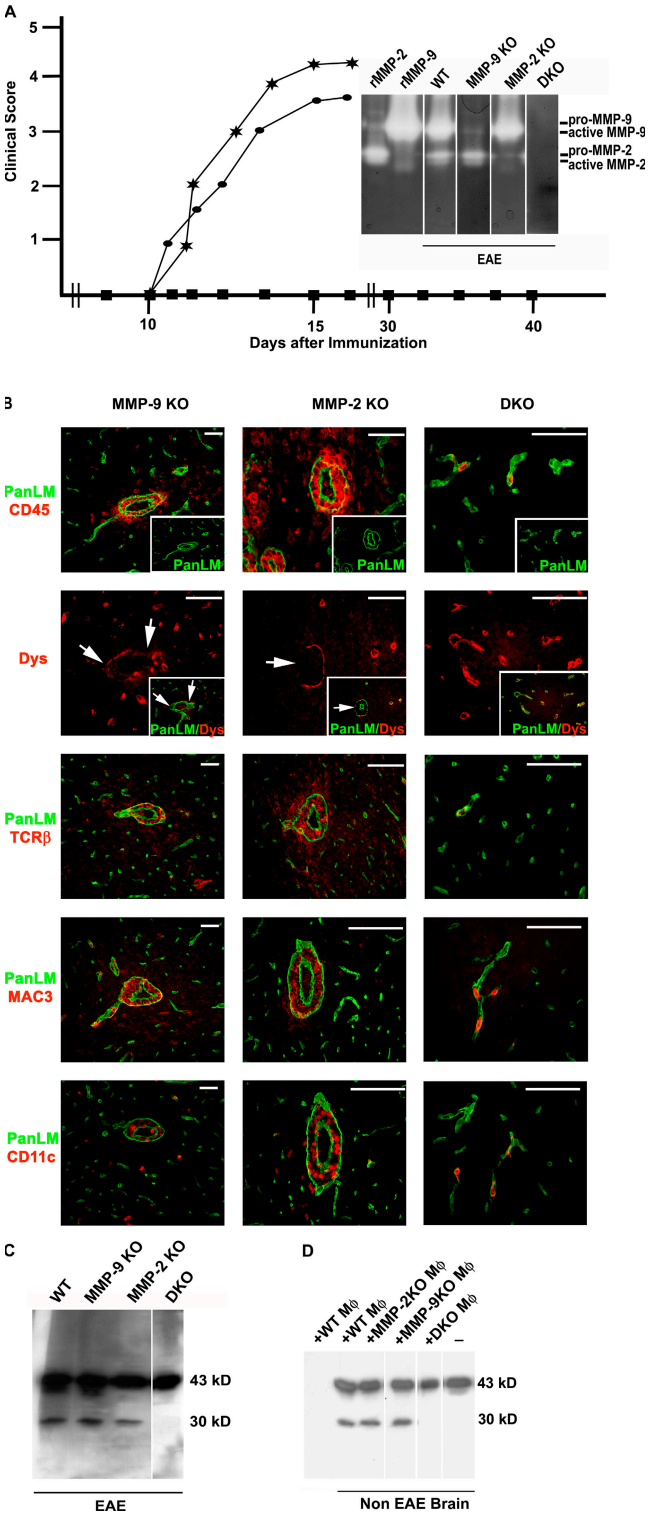

Figure 9. Combined MMP-2 and MMP-9 activity are crucial for EAE. (A) EAE progresses normally in MMP-2 KO (★) and MMP-9 KO (●), whereas MMP-2 and MMP-9 DKO (■) mice are resistant to EAE up to 40 d after MOG immunization. The inset gel zymograph compares gelatinases in CNS extracts from EAE-induced WT, MMP-2 KO, MMP-9 KO, and DKO mice. (B) All sections were stained for pan-laminin (green) and either CD45, T cell receptor (TCRβ), macrophage/microglia (MAC3), DC (CD11c), or β-dystroglycan, revealing normal cellular infiltrates and associated loss of β-dystroglycan in MMP-2 KO and MMP-9 KO mice (arrows), but not in DKO mice. Images are from different specimens and represent results from eight mice for each of the single KO mice and five DKO mice. (C) Western blot confirms the presence of the 30-kD β-dystroglycan fragment in the CNS of WT, MMP-2 KO, and MMP-9 KO, but not DKO mice. (D) Incubation of brain extracts from healthy mice (non-EAE) with macrophage-conditioned media (Mϕ) from MMP-2 KO, MMP-9 KO, or WT littermates, but not MMP-2/MMP-9 DKO, cleaves β-dystroglycan to the 30-kD fragment. Mϕ alone did not contain intact or cleaved β-dystroglycan. Bars, 40 μm.

been identified as an in vivo substrate of MMP-9 is NG2 proteoglycan, which accumulates in the CNS parenchyma as a result of demyelination insults, and retards maturation and differentiation of oligodendrocytes that are required for remyelination (18). Unlike dystroglycan, NG2 does not occur at the parenchymal BM-astrocyte endfeet border, but rather within the brain parenchyma surrounding oligodendrocytes. The dystroglycan complex links the parenchymal BM to the cytoskeleton of the astrocyte endfeet and disruptions to these interactions, by targeted elimination of dystroglycan (12) or changes in its glycosylation, cause severe neuronal defects (38). Interestingly, targeted elimination of dystroglycan in the CNS results in an inflammatory gliosis (12), which is consistent with a role for dystroglycan-mediated interactions as barriers to the movement of leukocytes, as suggested by the data here.

Cleavage of β-dystroglycan into a 30-kD fragment has been previously reported for both tumor and nontransformed cells (29, 39, 40) and can be mediated by MMPs, ADAMs, serine proteases, or a combination of these proteases, depending on tissue type (29, 39, 40). A cleavage site has been localized to the NH_2-terminal extracellular portion of β-dystroglycan, resulting in the loss of the α-dystroglycan binding domain and retention of a 30-kD COOH-terminal fragment anchored within the cell membrane (29, 39). Data presented here suggest that the same occurs at the astrocyte endfeet. In other tissues, α- and β-dystroglycan have been shown to remain nonconvalently associated through the binding of the COOH terminus of α-dystroglycan to the NH_2 terminus of β-dystroglycan even after cleavage (9, 29). In EAE brain, Western blots revealed the normal 120-kD α-dystroglycan subunit and no larger complexes, indicating that the cleaved ectodomain of β-dystroglycan is not associated with α-dystroglycan and, therefore, probably results in the release of α-dystroglycan from the cell surface. As α-dystroglycan represents the binding portion of the receptor complex and as astrocyte endfeet are still present at sites where dystroglycan is cleaved, this probably results in loss of anchorage sites to the parenchymal BM. Whether the released α-dystroglycan remains associated with the adjacent BM could not be determined as the result of the absence of appropriate antibodies. Its potential persistence in the parenchymal BM may convey additional signals to the infiltrating leukocytes or may alter the structural properties of the parenchymal

BM and thereby alter its stability and/or permeability. In the skin, such dystroglycan cleavage processes are physiological and probably represent a mechanism for basal keratinocyte detachment from the dermal-epidermal BM required for their differentiation (29). In contrast, astrocyte endfeet anchorage to the parenchymal BM is firm and long-term, and only in pathological cases such as inflammation is this cleavage process induced. It is likely that this MMP-mediated cleavage of β-dystroglycan represents a means of honing cell–matrix interactions required, for example, for cell movement or repair processes.

Data presented here indicate that MMP-2 and MMP-9 have complementary roles in β-dystroglycan cleavage in EAE. Our EAE experiments in MMP-9 KO mice are consistent with previous studies (22). However, the absence of differences between MMP-2 KO mice and +/− or WT littermates in the onset of EAE or disease severity contrasts with a recent study that reported increased susceptibility to EAE (41). A notable difference between the latter study and most other EAE studies is the unusually late onset of EAE symptoms in the WT mice (day 20) (41), whereas MMP-2 KO mice show onset of symptoms at ∼day 10 as reported here for both MMP-2 KO mice and their WT littermates. We have confirmed our findings on the MMP-2 KO mice in WT mice in which MMP-2 activity was eliminated through the use of a specific MMP-2 inhibitor (42) (unpublished data). As susceptibility to EAE by MOG immunization is influenced by genetic background, this is the most likely explanation for the discrepancy in the data. The absence of β-dystroglycan cleavage in the DKO mice, together with the clinical changes, indicates that this cleavage is a significant event in leukocyte infiltration to the CNS parenchyma. However, whether this cleavage is the cause or an effect of clinical EAE induction cannot be determined from the data present here. Current studies aim at in vivo inhibition of β-dystroglycan cleavage via point mutation of the cleavage site and subsequent EAE susceptibility studies to investigate this possibility. Furthermore, the data generated from the DKO mice suggest that loss of MMP-2 and MMP-9 has effects independent of dystroglycan cleavage and before endothelial cell transmigration because, as in the macrophage-depleted mice, leukocytes did not accumulate in the perivascular space. It has been suggested that MMP-9 and MMP-2 affect T cell activation in different manners (43, 44). However, the absence of significant changes in EAE onset or severity seen here in single KO mice and unpublished data from our laboratory on DKO indicate that this is not a significant issue in the EAE model used. The basis for the absence of a perivascular infiltrate in DKO mice is currently being examined.

In conclusion, our results confirm that leukocytes use different mechanisms for penetration of the endothelial cell monolayer and BM and the parenchymal BM and glia limitans, with gelatinase activity being required for the latter step. We have demonstrated that the activity of MMP-2 or MMP-9 is essential for EAE induction and have identified β-dystroglycan as a novel in vivo substrate for these gelatinases at the BBB. Collectively, the data suggest that gelatinase inhibition may protect against damage to the brain parenchyma by arresting the leukocytes infiltration.

MATERIALS AND METHODS

Animals

All mice were on a C57BL/6 background. MMP-2 KO mice (N11) were from the Institute of Physical and Chemical Research BRC, Japan (45), and MMP-9 KO mice (N9) were described previously (22). MMP-2 KO mice were bred with MMP-9 KO mice to generate DKO and heterozygous littermate controls. Experiments were conducted according to Animal Welfare guidelines.

MMPs and inhibitors

Inhibitors (Sigma-Aldrich) used were the following: 0.5M 4-(2-aminoethyl) benzenesulfonly fluoride hydrochloride (AEBSF), broad range serine protease inhibitor; 1 μM aprotinin, general serine protease inhibitor; 10 μM trans-epoxysuccinyl-L-leucylamido-(4-guanidino) butane (E-64), general cysteine protease inhibitor; and 0.5 mM 1,10-phenanthroline, general metalloproteinase inhibitor. Tissue inhibitors of matrix metalloproteinase (TIMP), TIMP-1, and TIMP-4 (R&D Systems) were used as MMP inhibitors that do not affect the activity of ADAMS or TACE. p-Aminophenylmercuric acetate (APMA) (Sigma-Aldrich) was used to activate rMMP-1, rMMP-7, and rMMP-8 (R&D Systems).

Experimental protocols

EAE. EAE was induced using the 35–55 peptide of MOG (5). Neurological defects were scored as stages 1 (flaccid tail), 2 (hind limb weakness), 3 (severe hind limb weakness), 4 (hind quarter paralysis), and 5 (forelimb weakness). CNS samples were collected at different stages and frozen in Tissue-Tek (Sakura Finetek) for immunofluorescence and in situ zymography, or snap frozen for Western blot and gel zymography.

Macrophage depletion. Liposomes containing clodronate or PBS, a gift from Roche Diagnostics GmbH, were injected i.v. (200 μl/mouse) at days 3, 7, and 9 after MOG immunization (13). Immunofluorescence, T cell proliferation assays, and FACS analyses were performed at days 10, 15, 19, and 21 after immunization.

T cell proliferation assay. T cells were isolated from draining LN, placed in RPMI 1640/5% FCS, and β-mercaptoethanol together with splenic DCs (from a nonimmunized mouse) and MOG 35–55 (0–100 μg/ml) or anti-CD3 (0–1 μg/ml), and incubated at 37°C for 3 d. Cell proliferation was determined by [^{3}H]thymidine incorporation.

FACS. Mice were perfused with PBS before spleens, LN, and brains were harvested. Spleens and LN were treated with 10 U type II collagenase (Roche) and 500 U DNase I (Sigma-Aldrich) and total cells were isolated by cell sieving (70 μm). Brain homogenates were separated into neuronal and leukocyte populations by discontinuous density gradient centrifugation using isotonic Percoll (GE Healthcare) (31). FACS was performed using a FACS Calibur (Becton Dickinson) with the antibodies indicated in Table I.

Macrophage and astrocyte cultures. Purified astrocyte cultures were generated from cerebral cortices of newborn mice and test cultures stained with anti-GFAP (Table I) to ascertain purity.

Mice were injected i.p. with 4% Brewers thioglycollate (Sigma-Aldrich), macrophages were harvested by peritoneal lavage and cultured to confluency in DMEM-F12/10% FCS.

Gel zymography. Crude CNS extracts were prepared by homogenization in ice-cold buffer (1 M NaH_2PO_4, 1 M sucrose, 0.5 M EDTA) with protease inhibitors (PI; Roche); samples were centrifuged and the solubilized fraction was collected. CNS extracts and conditioned media were prepurified by incubation with gelatin sepharose (46). Samples were separated on 10% polyacrylamide

gels containing 1 mg/ml gelatin under nonreducing conditions. Gels were washed in TBS, 25% Triton X-100, followed by TBS, 5 mM $CaCl_2$, 0.02% Brij 35 and incubated overnight in the same buffer. Gels were stained with Coomassie blue and destained in acetic acid: methanol: dH_2O [10:50:40].

In situ zymography and immunofluorescence. MMP activity was localized in brain sections using a modified method of Oh et al. (47), which, in contrast with classical in situ zymography, does not require separation of the substrate from the underlying tissue section, permitting costaining of the section and precise cellular localization of MMP activity. 10 μg/ml DQ-gelatin or DQ-type IV collagen (EnzCheck; Invitrogen) in 50 mM Tris-HCl, pH 7.4, plus 1 mM $CaCl_2$ was applied to CNS cryosections, in the presence or absence of 1,10-phenanthroline. Slides were incubated for 6 h in a humid chamber at 37°C, washed in PBS, and fixed in −20°C methanol before immunofluorescence staining (5). Digestion of the DQ-gelatin results in unquenching of fluorochrome, which was detected with excitation at 460–500 nm and emission at 512–542 nm.

Primary antibodies used in in situ zymography coupled with immunofluorescence or immunofluorescence alone are listed in Table I. Bound antibodies were visualized using FITC- or Texas red–conjugated goat anti–rat, and rhodamine- or Pacific blue–conjugated anti–rabbit secondary antibodies (Jackson ImmunoResearch Laboratories and Invitrogen).

Sections were examined using a Zeiss Axiophot microscope equipped with epifluorescent optics and documented using a Hamamatsu ORCA1 camera and Openlab software (Improvision).

Western blots: wheat germ agglutinin-glycoprotein extraction. Cell/tissue extracts were homogenized in TBS containing 1% Triton X-100 and PI, and solubilized by rotation at 4°C. KCl-washed membrane fractions were prepared from solubilized CNS extracts. Glycoproteins were enriched using wheat germ agglutinin (WGA) beads (Vector Laboratories) and used in dystroglycan Western blots. In some cases, extracted glycoproteins from noninflamed CNS or from astrocyte cultures were incubated overnight with rMMP-3-activated rMMP-2 or rMMP-9, or with APMA-activated rMMP-1, rMMP-7, or rMMP-8, before use in Western blots. Although rMMP-3 and APMA are both capable of activating rMMP-2 and rMMP-9, MMP-3 is more efficient and was therefore used. rMMP-2 and rMMP-9 activation with APMA results in the same pattern of results.

Samples were separated by SDS-PAGE on 3–12% gradient gels, transferred to PVDF membranes (GE Healthcare), and Western blots were performed using the antibodies indicated in Table I.

The authors thank R. Hallmann, J. Van Damme, and P. Van den Steen for helpful discussions and G. Roos for technical assistance.

This work was supported by the German (grant nos. So285/5-1, So285/5-2) and Swedish Research Councils (grant nos. K2005-06X-14184-04A, 621-2001-2142), Alfred Österlunds, Knut and Alice Wallenbergs (grant no. 2002.0056), the Greta and Johan Kocks Foundations, the Fund for Scientific Research-Flanders, the "Geconcerteerde OnderzoeksActies," and the Charcot Foundation, Belgium.

The authors have no conflicting financial interests.

Submitted: 6 July 2005
Accepted: 9 March 2006

REFERENCES

1. Wolf, K., R. Muller, S. Borgmann, E.B. Brocker, and P. Friedl. 2003. Amoeboid shape change and contact guidance: T-lymphocyte crawling through fibrillar collagen is independent of matrix remodeling by MMPs and other proteases. *Blood*. 102:3262–3269.
2. Yadav, R., K.Y. Larbi, R.E. Young, and S. Nourshargh. 2003. Migration of leukocytes through the vessel wall and beyond. *Thromb. Haemost*. 90:598–606.
3. Engelhardt, B. 1997. Lymphocyte trafficking through the central nervous system. *In* Adhesion Molecules and Chemokines in Lymphocyte Trafficking. A. Hamann, editor. Harwood Academic Publishers, Amsterdam. 173–200.
4. Kawakami, N., U.V. Nagerl, F. Odoardi, T. Bonhoeffer, H. Wekerle, and A. Flugel. 2005. Live imaging of effector cell trafficking and autoantigen recognition within the unfolding autoimmune encephalomyelitis lesion. *J. Exp. Med*. 201:1805–1814.
5. Sixt, M., B. Engelhardt, F. Pausch, R. Hallmann, O. Wendler, and L.M. Sorokin. 2001. Endothelial cell laminin isoforms, laminin 8 and 10, play decisive roles in T-cell recruitment across the blood-brain-barrier in an EAE model. *J. Cell Biol*. 153:933–945.
6. Reese, T., and M. Karnovsky. 1967. Fine structure localization of a blood-brain barrier to endogenous peroxidase. *J. Cell Biol*. 34:207–217.
7. Tian, M., C. Jacobson, S.H. Gee, K.P. Campbell, S. Carbonetto, and M. Jucker. 1996. Dystroglycan in the cerebellum is a laminin α2-chain binding protein at the glial-vascular interface and is expressed in Purkinje cells. *Eur. J. Neurosci*. 8:2739–2747.
8. Zaccaria, M.L., F. Di Tommaso, A. Brancaccio, P. Paggi, and T.C. Petrucci. 2001. Dystroglycan distribution in adult mouse brain: a light and electron microscopy study. *Neuroscience*. 104:311–324.
9. Durbeej, M., M. Henry, and K.P. Campbell. 1998. Dystroglycan in development and disease. *Curr. Opin. Cell Biol*. 10:594–601.
10. Talts, J.F., Z. Andac, W. Göhring, A. Brancaccio, and R. Timpl. 1999. Binding of G domains of laminin α1 and α2 chains and perlecan to heparin, sulfatides, α-dystroglycan and several extracellular matrix proteins. *EMBO J*. 18:863–870.
11. Sugita, S., F. Saito, J. Tang, J. Satz, K. Campbell, and T.C. Sudhof. 2001. A stoichiometric complex of neurexins and dystroglycan in brain. *J. Cell Biol*. 154:435–445.
12. Moore, S.A., F. Saito, J. Chen, D.E. Michele, M.D. Henry, A. Messing, R.D. Cohn, S.E. Ross-Barta, S. Westra, R.A. Williamson, et al. 2002. Deletion of brain dystroglycan recapitulates aspects of congenital muscular dystrophy. *Nature*. 418:422–425.
13. Tran, E.H., K. Hoekstra, N. v. Rooijen, C.D. Dijkstra, and T. Owens. 1998. Immune evasion of the CNS parenchyma and experimental allergic encephalomyelitis, but not leukocyte extravasation from blood, are prevented in macrophage-depleted mice. *J. Immunol*. 161:3767–3775.
14. Körner, H., D.S. Riminton, D.H. Strickland, F.A. Lemckert, J.D. Pollard, and J.D. Sedgwick. 1997. Critical points of tumor necrosis factor action in CNS autoimmune inflammation defined by gene targeting. *J. Exp. Med*. 186:1585–1590.
15. Grewal, I.S., H.G. Foellmer, K.D. Grewal, H. Wang, W.P. Lee, D. Tumas, C.A. Janeway Jr., and R.A. Flavell. 2001. CD62L is required on effector cells for local interactions in the CNS to cause myelin damage in experimental allergic encephalomyelitis. *Immunity*. 14:291–302.
16. Graesser, D., S. Mahooti, and J. Madri. 2000. Distinct roles for MMP-2 and α4 integrin in autoimmune T cell extravsastion and residency in brain parenchyma during EAE. *J. Neuroimmunol*. 109:121–131.
17. Gijbels, K., P. Proost, S. Masure, H. Carton, A. Billiau, and G. Opdenakker. 1993. Gelatinase B is present in the cerebrospinal fluid during EAE and cleaves myelin basic protein. *J. Neurosci. Res*. 36:432–440.
18. Larsen, P.H., J.E. Wells, W.B. Stallcup, G. Opdenakker, and V.W. Yong. 2003. MMP-9 facilitates remyelination in part by processing the inhibitory NG2 proteoglycan. *J. Neurosci*. 23:11127–11135.
19. Van den Steen, P.E., P. Proost, A. Wuyts, J. Van Damme, and G. Opdenakker. 2000. Neutrophil gelatinase B potentiates interleukin-8 tenfold by aminoterminal processing, whereas it degrades CTAP-III, PF-4, and GRO-alpha and leaves RANTES and MCP-2 intact. *Blood*. 96:2673–2681.
20. McQuibban, G.A., J.H. Gong, E.M. Tam, C.A. McCulloch, I. Clark-Lewis, and C.M. Overall. 2000. Inflammation dampened by gelatinase A cleavage of monocyte chemoattractant protein-3. *Science*. 289:1202–1206.
21. Gearing, A.J., P. Beckett, M. Christodoulou, M. Churchill, J. Clements, A.H. Davidson, A.H. Drummond, W.A. Galloway, R. Gilbert, J.L. Gordon, et al. 1994. Processing of TNF-α precursor by metalloproteinases. *Nature*. 370:555–557.
22. Dubois, B., S. Masure, U. Hurtenbach, L. Paemen, H. Heremans, J. van der Oord, R. Sciot, T. Meinhardt, G. Hämmerling, G. Opdenakker, and B. Arnold. 1999. Resistance of young gelatinase B-deficient mice to EAE and necrotizing tail lesions. *J. Clin. Invest*. 104:1507–1515.

23. Kieseier, B.C., R. Kiefer, J.M. Clements, K. Miller, G.M. Wells, T. Schweitzer, A.J. Gearing, and H.P. Hartung. 1998. MMP-9 and -7 are regulated in EAE. *Brain*. 121:159–166.
24. Nygardas, P., and A. Hinkkanen. 2002. Up-regulation of MMP-8 and MMP-9 activity in the BALB/c mouse spinal cord correlates with the severity of EAE. *Clin. Exp. Immunol*. 128:245–254.
25. Gijbels, K., R.E. Galardy, and L. Steinman. 1994. Reversal of EAE with a hydroxamate inhibitor of MMPs. *J. Clin. Invest*. 94:2177–2182.
26. Hewson, A.K., T. Smith, J.P. Leonard, and M.L. Cuzner. 1995. Suppression of experimental allergic encephalomyelitis in the Lewis rat by the MMP inhibitor Ro31-9790. *Inflamm. Res*. 44:345–349.
27. Kjeldsen, L., D.F. Bainton, H. Sengelov, and N. Borregaard. 1993. Structural and functional heterogeneity among peroxidase-negative granules in human neutrophils: identification of a distinct gelatinase-containing granule subset by combined immunocytochemistry and subcellular fractionation. *Blood*. 82:3183–3191.
28. Moll, J., P. Barzaghi, S. Lin, G. Bezakova, H. Lochmuller, E. Engvall, U. Muller, and M.A. Ruegg. 2001. An agrin minigene rescues dystrophic symptoms in a mouse model for congenital muscular dystrophy. *Nature*. 413:302–307.
29. Herzog, C., C. Has, C.W. Franzke, F.G. Echtermeyer, U. Schlotzer-Schrehardt, S. Kroger, E. Gustafsson, R. Fässler, and L. Bruckner-Tuderman. 2004. Dystroglycan in skin and cutaneous cells: β-subunit is shed from the cell surface. *J. Invest. Dermatol*. 122:1372–1380.
30. Parks, W.C., C.L. Wilson, and Y.S. Lopez-Boado. 2004. MMPs as modulators of inflammation and innate immunity. *Nat. Rev. Immunol*. 4:617–629.
31. Ford, A.L., A.L. Goodsall, W.F. Hickey, and J.D. Sedgwick. 1995. Normal adult ramified microglia separated from other CNS macrophages by flow cytometric sorting. *J. Immunol*. 154:4309–4321.
32. Nikolic, T., S. Geutskens, N. Van Rooijen, H. Drexhage, and P. Leenan. 2005. Dendritic cells and macrophages are essential for the retention of lymphocytes in (peri)-insulitis of the nonobese diabetic mouse: a phagocyte depletion study. *Lab. Invest*. 85:487–501.
33. Teesalu, T., A.E. Hinkkanen, and A. Vaheri. 2001. Coordinated induction of extracellular proteolysis systems during EAE in mice. *Am. J. Pathol*. 159:2227–2237.
34. Archambault, A.S., J. Sim, M.A. Gimenez, and J.H. Russell. 2005. Defining antigen-dependent stages of T cell migration from the blood to the CNS parenchyma. *Eur. J. Immunol*. 35:1076–1085.
35. Flügel, A., T. Berkowicz, T. Ritter, M. Labeur, D.E. Jenne, Z. Li, J.W. Ellwart, M. Willem, H. Lassmann, and H. Wekerle. 2001. Migratory activity and functional changes of green fluorescent effector cells before and during EAE. *Immunity*. 14:547–560.
36. Greter, M., F.L. Heppner, M.P. Lemos, B.M. Odermatt, N. Goebels, T. Laufer, R.J. Noelle, and B. Becher. 2005. Dendritic cells permit immune invasion of the CNS in an animal model of multiple sclerosis. *Nat. Med*. 11:328–334.
37. Tam, E.M., C.J. Morrison, Y.I. Wu, M.S. Stack, and C.M. Overall. 2004. Membrane protease proteomics: isotope-coded affinity tag MS identification of undescribed MT1-MMP substrates. *Proc. Natl. Acad. Sci. USA*. 101:6917–6922.
38. Montanaro, F., and S. Carbonetto. 2003. Targeting dystroglycan in the brain. *Neuron*. 37:193–196.
39. Yamada, H., F. Saito, H. Fukuta-Ohi, D. Zhong, A. Hase, K. Arai, A. Okuyama, R. Maekawa, T. Shimizu, and K. Matsumura. 2001. Processing of β-dystroglycan by MMP disrupts the link between the extracellular matrix and cell membrane via the dystroglycan complex. *Hum. Mol. Genet*. 10:1563–1569.
40. Singh, J., Y. Itahana, S. Knight-Krajewski, M. Kanagawa, K.P. Campbell, M.J. Bissell, and J. Muschler. 2004. Proteolytic enzymes and altered glycosylation modulate dystroglycan function in carcinoma cells. *Cancer Res*. 64:6152–6159.
41. Esparza, J., M. Kruse, J. Lee, M. Michaud, and J.A. Madri. 2004. MMP-2 null mice exhibit an early onset and severe EAE due to an increase in MMP-9 expression and activity. *FASEB J*. 18:1682–1691.
42. Matsumura, S., S. Iwanaga, S. Mochizuki, H. Okamoto, S. Ogawa, and Y. Okada. 2005. Targeted deletion or pharmacological inhibition of MMP-2 prevents cardiac rupture after myocardial infarction in mice. *J. Clin. Invest*. 115:559–609.
43. Fernandez, F.G., L.G. Campbell, W. Liu, J.M. Shipley, S. Itohara, G.A. Patterson, R.M. Senior, T. Mohanakumar, and A. Jaramillo. 2005. Inhibition of obliterative airway disease development in murine tracheal allografts by MMP-9 deficiency. *Am. J. Transplant*. 5:671–683.
44. Campbell, L.G., S. Ramachandran, W. Liu, J.M. Shipley, S. Itohara, J.G. Rogers, N. Moazami, R.M. Senior, and A. Jaramillo. 2005. Different roles for MMP-2 and MMP-9 in the pathogenesis of cardiac allograft rejection. *Am. J. Transplant*. 5:517–528.
45. Itoh, T., T. Ikeda, H. Gomi, S. Nakao, T. Suzuki, and S. Itohara. 1997. Unaltered secretion of β-amyloid precursor protein in gelatinase A (MMP-2)-deficient mice. *J. Biol. Chem*. 272:22389–22392.
46. Dubois, B., S. Masure, U. Hurtenbach, L. Paemen, H. Heremans, J. van den Oord, R. Sciot, T. Meinhardt, G. Hammerling, G. Opdenakker, and B. Arnold. 1999. Resistance of young gelatinase B-deficient mice to EAE and necrotizing tail lesions. *J. Clin. Invest*. 104:1507–1515.
47. Oh, L.Y., P.H. Larsen, C.A. Krekoski, D.R. Edwards, F. Donovan, Z. Werb, and V.W. Yong. 1999. MMP-9/gelatinase B is required for process outgrowth by oligodendrocytes. *J. Neurosci*. 19:8464–8475.
48. Eusebio, A., F. Oliveri, P. Barzaghi, and M.A. Ruegg. 2003. Expression of mouse agrin in normal, denervated and dystrophic muscle. *Neuromuscul. Disord*. 13:408–415.
49. Gawlik, K., Y. Miyagoe-Suzuki, P. Ekblom, S. Takeda, and M. Durbeej. 2004. Laminin α1 chain reduces muscular dystrophy in laminin α2 chain deficient mice. *Hum. Mol. Genet*. 13:1775–1784.